Evidence of wildfire smoke in surface water of an unburned watershed

Joshua S. Evans[1], Ann-Lise Norman[1,2], Mary L. Reid[1,3,*]

[1] Environmental Science Program, University of Calgary, Calgary, AB, Canada

[2] Department of Physics and Astronomy, University of Calgary, Calgary, AB, Canada, orcid.org/0000-0002-5430-7409

[3] Department of Biological Sciences, University of Calgary, Calgary, AB, Canada; orcid.org/0000-0002-7679-1967

* Corresponding author: M.L. Reid, Dept. of Biological Sciences, University of Calgary, Calgary, Alberta, T2N 1N4 Canada, Email: mreid@ucalgary.ca

Key Points

- An 18-year water monitoring study with six smoke years revealed that smoke from distant fires affects water chemistry.
- Smoke was traced from wildfire activity to air and rain chemistry to river water chemistry using potassium as a marker.
- Potassium can be a sentinel ion to detect smoke in the water across broad geographic areas far from wildfires.

Abstract Large wildfires generate smoke that greatly compromises air quality over a wide area. Limited studies have suggested that smoke constituents may enter natural water bodies. In an 18-year water monitoring study, we examined whether smoke from distant wildfires had a detectable effect on ion content in a mountain river in an unburned watershed. Significant local wildfire smoke occurred in six years as traced by MODIS satellite data of fires, regional and local atmospheric fine particulate matter ($PM_{2.5}$), and the amount of potassium (K^+) in $PM_{2.5}$ as a marker of vegetation combustion. Rainwater had elevated K^+ and calcium (Ca^{2+}, also associated with wildfire smoke) in smoke years compared to no-smoke years, and was the primary route of atmospheric deposition. Similarly, river water in smoke years had elevated concentrations of K^+ and Ca^{2+}, with a higher ratio of K^+ to Ca^{2+} compared to no-smoke years. River concentrations were generally unrelated to river discharge and observed K^+ concentrations in smoke and no-smoke years could be accounted for atmospheric deposition. Our study provides early evidence that wildfires affect water quality far beyond the watersheds where they occur. Wildfires are increasing in frequency and extent worldwide, widely distributing vast quantities of smoke containing nutrients, toxins and microbes. Potassium is a routinely-measured water quality parameter that can act as a sentinel of smoke inputs. Further work is needed on the patterns and processes by which wildfire smoke enters water as well as on the consequences for ecosystems and human health.

Keywords 1871 Surface water quality, 1879 Watershed, 0345 Pollution: urban and regional

1. Introduction

Wildfires cause major alterations to the biogeochemistry of ecosystems and are anticipated to increase in frequency and intensity with climate change (Dupuy *et al.*, 2020; Halofsky *et al.*, 2020; Smith *et al.*, 2020). For fires within watersheds, the biogeochemical effects of wildfires are evident in surface water quality as a result of runoff of nutrients and toxins generated directly by combustion of vegetation or through reductions in uptake by vegetation (Nunes *et al.*, 2017; Robinne *et al.*, 2019; Santín *et al.*, 2015). Another potential route of surface water contamination from wildfire may be smoke, an acknowledged but rarely studied process (Dokas *et al.*, 2007; Spencer and Hauer, 1991). Here, we test for evidence of smoke in a mountain river within an unburned watershed using natural variation in wildfire smoke across 18 years of water sampling.

Wildfire smoke consists of fine particulate matter ($PM_{2.5}$) derived from biomass combustion (Schweizer *et al.*, 2019). Smoke can be transported thousands of kilometers (Duck *et al.*, 2007; Hung *et al.*, 2020) and persist for months (Yu *et al.*, 2019). It contains a wide variety of chemicals, many of which are toxic (Berthiaume *et al.*, 2020; Gilman *et al.*, 2015; Verma *et al.*, 2009), as well as living microbes (Moore *et al.*, 2021). These have consequences at many scales from individual firefighters to ecosystems. $PM_{2.5}$ is routinely monitored as part of air quality measurements and derives from many sources. In western North America, wildfires contribute more than 70% of the total $PM_{2.5}$ on days exceeding regulatory $PM_{2.5}$ standards (Liu *et al.*, 2016; Mirzaei *et al.*, 2018).

Potassium, K^+, is a marker of wildfire smoke that is also routinely measured as a base cation in water quality studies. Water-soluble K^+ in $PM_{2.5}$ is almost exclusively from vegetation burning

(Munchak *et al.*, 2011; Sullivan *et al.*, 2008; Valerino *et al.*, 2017) as a result of its relatively low volatilization temperature of 774°C (Raison *et al.*, 1985). Potassium is also associated with weathering of K-bearing minerals such as feldspars. As a limiting plant nutrient , its concentration varies little with stream discharge in forested ecosystems (Tripler *et al.*, 2006). Calcium, Ca^{2+}, is also associated with wildfire smoke (Sillanpää *et al.*, 2005), and is transported as fine ash (Raison *et al.*, 1985) but another common source in watersheds is the weathering of carbonate rocks.

We tested for smoke inputs into the Kananaskis River in southwest Alberta, Canada. The Kananaskis River is a small mountain river that is part of the larger watershed that provides drinking water to 60% of residents of the City of Calgary (population 1.5 million); the remainder of Calgary's drinking water comes from the neighboring Elbow River watershed. There were no wildfires within the Kananaskis River watershed during our study, but there were several smoky years from distant fires. For each year, we determined the wildfire extent and intensity, the quantity and chemical composition of atmospheric $PM_{2.5}$ and rainwater, and the river's concentrations of K^+ and Ca^{2+}. Variation in K^+ was assumed to be due to smoke, while variation in Ca^{2+} might have both smoke and weathering sources. Our scale of comparison was annual, comparing smoke years with other years. We predicted that concentrations of K^+ would be higher in smoke years if smoke was entering the surface water, likely to a greater extent than would Ca^{2+} concentrations.

2. Methods

2.1 Study area

The Kananaskis River watershed (930 km^2) is located in the eastern slopes of the Rocky Mountains of southwest Alberta, Canada (50.9^{o}N, 115.1^o W), originating at the continental divide at the border of Alberta and British Columbia (3500 m a.s.l) and discharging into the Bow River (1290 m a.s.l.). Bedrock in the Kananaskis Valley is composed of calcium-rich limestone, sandstone, siltstone, carbonates and shales that is overlain by alluvium up to 40 m deep in the midsection of the lower Kananaskis River (McMechan, 1995). Feldspars and other K-bearing minerals are present in bedrock and weathering contributes carbonate and K^+ to glacier-fed streams reflecting long-term water-rock interactions (Sharp *et al.*, 2002). The climate is cool and dry: mid-summer mean daily temperature is 13^{o}C and yearly precipitation is 634 mm; most precipitation is in May and June (208 mm) while July and August have an average of 130 mm of rain collectively (Whitfield, 2014). The valley contains montane, sub-alpine, and alpine ecoregions with montane forests at lower elevations that are dominated by lodgepole pine (*Pinus contorta)*, white spruce (*Picea glauca*), and trembling aspen (*Populus tremuloides*) (Crosby, 1990). The Kananaskis watershed is protected from development other than for non-motorized recreation.

The lower section of the river, where our study was conducted, originates at a hydroelectric dam (1680 m a.s.l.) at Lower Kananaskis Lake that is in turn fed via a hydroelectric dam by Upper Kananaskis Lake with a total catchment of 315 km^2 (Crosby, 1990). Lower Kananaskis Lake is oligotrophic with concentrations of K^+ and Ca^{2+} of 0.29 mg/L ± 0.02 SE and 36.9 mg/L ± 0.4 SE, respectively (Crosby, 1990). The reservoir fills with water over spring and summer, with water

released for some hours each day over the summer for electricity generation (Alberta Government, 2021). We sampled Kananaskis River water in and around the Evan-Thomas Provincial Recreation Area (ETPRA), an area with outdoor recreation infrastructure. Sampling was conducted at two sites annually from 2002-2019 in late summer. The more upstream site, Opal (50.8330°N, 115.1688°W, 1542 m a.s.l.) was 17 km downstream of Lower Kananaskis Lake with an additional catchment of 170 km^2. Here, the river was 18 m wide and 0.3 m deep with a discharge of 2.8 m^3/s on average across years. Opal was adjacent to a small day-use area and upstream of the ETPRA. The second site was located 40 m upstream of the Kananaskis Village bridge (KVB, 50.9316°N, 115.1293°W, 1440 m a.s.l.). KVB was 12 km downstream of Opal with an additional catchment area of 240 km^2.

Years with notable ground-level wildfire smoke were identified anecdotally by the local newspaper as 2003, 2010, 2014 and 2015 (Calgary Herald, 2015) and additionally by our personal observations as 2017 and 2018. We quantified wildfire activity and air quality to substantiate these observations.

2.2 Wildfire activity

To quantify wildfire activity each summer, we obtained daily Fire Radiative Power (FRP, Watts m^{-2}) values, as detected by MODIS satellites, from NASA's Fire Information Resource Management System (NASA, 2020). The data consist of values for 1 x 1 km pixels in which non-zero FRP values were detected. We obtained FRP values for an area spanning British Columbia, western Alberta, northern Washington and Montana (Figure 1). This region was chosen as most of the smoke transported to the Kananaskis region during fire years comes from

British Columbia, with additional inputs from Washington and Montana (Mirzaei *et al.*, 2018). Coniferous forests dominate this region. As an index of biomass burnt in each year, we used the sum of FRP values for July and August in each year.

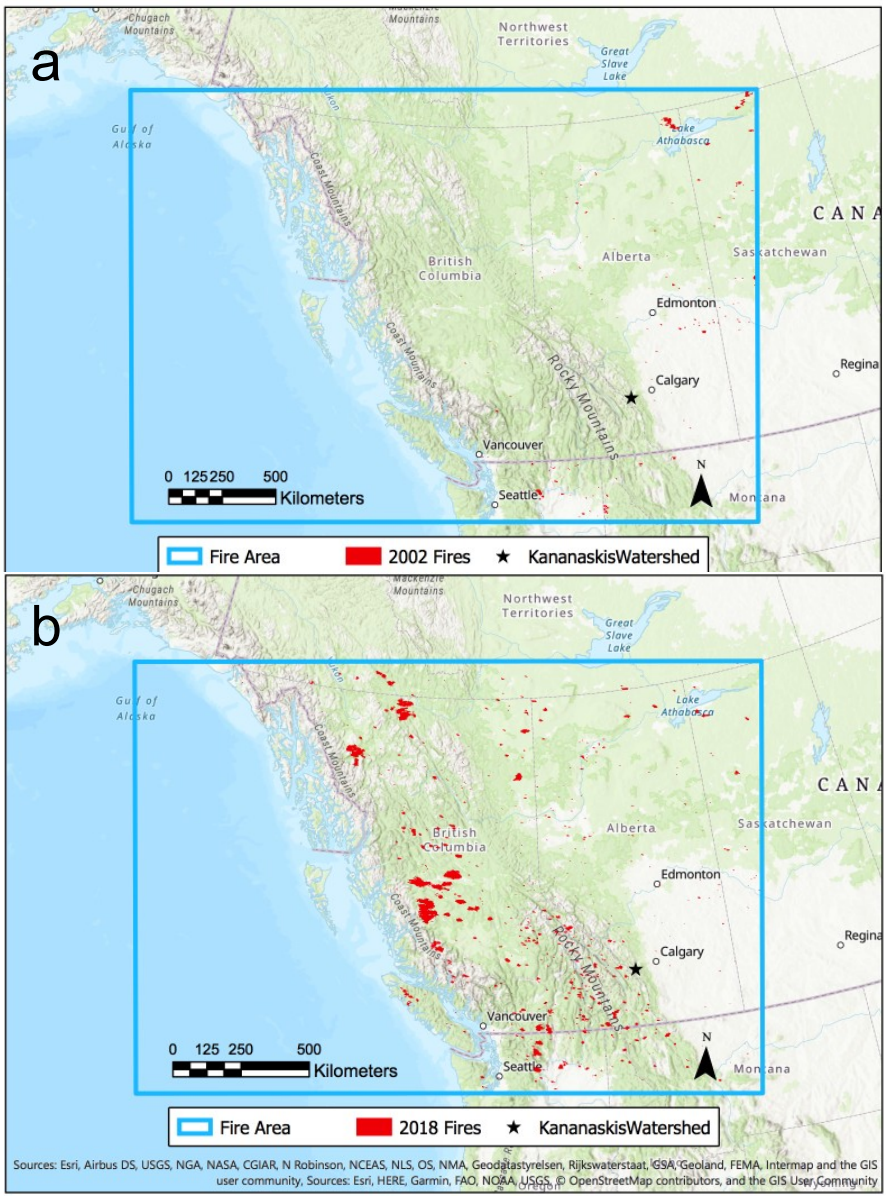

Figure 1. Area (blue box) for which wildfire activity was determined in northwestern North America with wildfires indicated for (a) 2002 that was not smoky and (b) 2018 that was a smoke year. Latitude 42.086 to 69.605, longitude -109.848 to -141.080.

2.2 Atmospheric particulate matter and chemistry

We obtained hourly $PM_{2.5}$ measurements for July and August of each year for the nearest long-term monitoring station (Open Calgary, 2021), located in northwest Calgary, Alberta, 70 km east of our study area. We used mean daily values for July and August. We also obtained atmospheric $PM_{2.5}$ and chemistry data within the lower Kananaskis Valley from the IMPROVE air monitoring program (IMPROVE (2021); Barrier Lake site, ID 94952, BALA1) that operated a station 12 km north of our KVB site from 2011-2017 at the University of Calgary Biogeoscience Institute's Barrier Lake Field Station. IMPROVE air samples were collected over 24 h, every three days. Of the physical and chemical attributes measured by IMPROVE, we focused on $PM_{2.5}$ and K^+ (note that Ca^{2+} was not available for this dataset) for July and August each year. These data pertain to dry deposition of atmospheric compounds.

2.3 Rainfall chemistry and quantity

For our study years of 2002-2019, we obtained rainfall chemistry and sample volume data from the Government of Alberta that operates a wet-only precipitation collector at the Barrier Lake Field Station in the Kananaskis Valley (51.027°, -115.034°). Accumulated precipitation was collected weekly (with some exceptions). We used data for sampling periods that ended in July or August to analyze K^+ and Ca^{2+} concentrations and wet deposition (data available at https://dataverse.scholarsportal.info/privateurl.xhtml?token=844fefbe-ac6e-4e37-800c-7a37301630e9). Some sample periods had missing data (excluding periods with no rain), so for wet deposition we standardized each year to 62 days. Daily total rainfall was also obtained from the Environment Canada weather station ("Kananaskis") at the Barrier Lake Field Station (Government of Canada, 2021).

2.4 River chemistry and hydrology

We collected grab water samples from our two sites on the Kananaskis River over two consecutive days each year; across years, sampling dates ranged from August 31 to September 7. We sampled from the main stem of the river after rinsing the sample bottle three times with river water at the sample site. Water samples were filtered using a 0.45µm cellulose nitrate filter into 1L polystyrene bottles. Samples were then analyzed for K^+ and Ca^{2+} using ion chromatography (no potassium data for 2004; all data available at University of Calgary Environmental Science Program (2020)). In most years we conducted four replicate analyses per site, ranging from 2-8 samples per site. We measured water discharge at the Opal site using the velocity-area method (cross-section sampling intervals 0.5, 1 or 2 m) each year except 2008, 2012, and 2013 (data available at https://dataverse.scholarsportal.info/privateurl.xhtml?token=844fefbe-ac6e-4e37-800c-7a37301630e9).

2.5 Statistical methods

Our primary response variables to track the processes by which smoke might enter water were FRP (fire activity), $PM_{2.5}$ quantity and composition (air quality), rainwater chemistry, and river chemistry. Our primary predictor variables were yearly smoke category (smoke, no-smoke) with year nested within smoke category. FRP, $PM_{2.5}$ and rain models also included month (July, August); the rainwater chemistry models further included sample volume. River chemistry analyses included sample site (Opal, KVB). The residuals for all statistical models were examined for conformity to normality and homoscedasticity and response variables were transformed as required. Analyses were completed using the statistical software R 4.0.2 (R Core

Team, 2018) and JMP 12.0.1 (SAS, 2015). Means are reported ± SE, most of which are least square means (LSMs) from models, back-transformed as needed.

2.6 Atmospheric deposition model

To evaluate whether the atmospheric inputs of K^+ were sufficient to account for the observed K^+ concentrations in the river, we estimated the dry and wet deposition of K^+ in smoke and no-smoke years. Dry deposition is a function of the concentration in the air, which we knew for six years including two smoke years, and of deposition velocity. Deposition velocity, V_d, of $PM_{2.5}$ can range from 0.03 cm/s for smooth surfaces such as bare rock to 10 cm/s or more for plant surfaces (Giardina and Buffa, 2018; Schaubroeck *et al.*, 2014). In our study area, the Kananaskis Valley is approximately 10% bare rock. Based on deposition velocities for pine forests (Schaubroeck *et al.*, 2014), we chose $V_d = 0.5$ cm/s as a moderate value for the whole watershed. To get the total amount of K^+ in dry deposition in the watershed between Opal and Lower Kananaskis Lake in July and August in smoke and no-smoke years, we multiplied together the observed LSMs of air concentration of K^+ (separately for smoke and no-smoke categories), V_d, the number of seconds in July and August, and the watershed area (170 km^2). Given this simple equation, adjusting the value of any component has a proportional effect on the estimated dry deposition. For wet deposition, we determined the mass of K^+ deposited in the watershed from the observed concentrations of K^+ in rain (LSMs for smoke, no-smoke) and the mean total rain in July and August of smoke and no-smoke years, separately, applied to the watershed area. We added dry and wet deposition to get total deposition of K^+ and determined the percent contributed by wet deposition. Total deposition reflects the sum of all deposition in July and August, so to distribute the deposition and its subsequent entry into the river across the summer,

213 we divided the total by 62 days. To predict the K^+ concentration in the river, we divided the
214 daily K^+ deposition by the estimated volume of the river between Lower Kananaskis Lake and
215 Opal. To estimate river volume, we multiplied the river width and mean depth that we measured
216 at Opal by the length of the river (17 km); because the river is larger at Opal than at its origin,
217 this is an over-estimate of river volume. River volume did not differ between smoke and no-
218 smoke years ($P > 0.5$), so we used the median calculated volume of all available years (85.55 *
219 10^6 L). We conducted sensitivity analyses for watershed area and river volume by varying the
220 base values by ± 10 and 30%; we also varied $PM_{2.5}$ deposition velocity, V_d, from 0.1 to 2 cm/s to
221 span most of the values estimated for forested areas reported by Giardina and Buffa (2018).
222

223 # 3. Results

224 ## 3.1 Wildfire activity

225 Wildfire activity varied greatly among years in our study (Figure 2a). The amount of fire,
226 measured as number of FRP pixels in July and August each year, ranged from 1,613 (2008) to
227 47,184 (2018), while the maximum FRP values in each year ranged from 2,120 to 14,377 Watts/
228 m^2; the number and maximum values of FRP were positively correlated ($r = 0.81$, $P < 0.0001$, N
229 = 18 years). The pre-assigned smoke years had higher FRP values than the other years (Table
230 1a). Within smoke categories, FRP values did not detectably differ among years, nor did July
231 and August values consistently differ (Table 1a). These results support the wildfire source of
232 smoke in our *a priori* classification of smoke and no-smoke years.

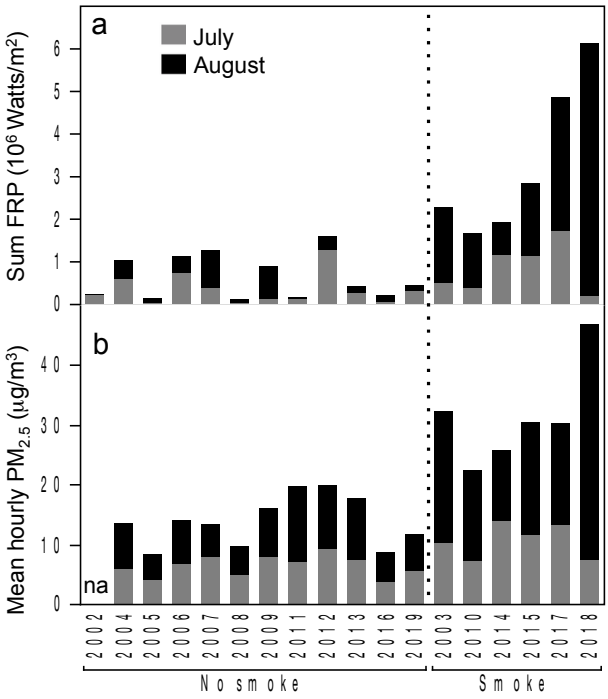

Figure 2. (a) Fire activity measured as summed Fire Radiative Power (FRP) and (b) mean hourly $PM_{2.5}$ in NW Calgary, Alberta, for July and August for the years of our study. Dotted vertical line distinguishes years with no smoke and with smoke based on *a priori* classification. na=not available.

Table 1. Linear model results for fire activity, air quality, rain chemistry and river chemistry. Year was nested within the Smoke categories. Significant P values are in bold.

		Effect tests		
Response / R^2	**Predictor**	**F**	**df**	**P**
a) Fire activity Watts/m²				
sum FRP [a]	Smoke	29.59	1,17	**< 0.0001**
$R^2 = 0.768$	Year[Smoke]	1.60	16,17	> 0.1
	Month	0.96	1,17	> 0.3
b) Air quality µg/m²				
$PM_{2.5}$ Calgary [a]	Smoke	40.62	1,16	**< 0.0001**
$R^2 = 0.809$	Year[Smoke]	1.31	15,16	> 0.2
	Month	7.46	1,16	**< 0.02**
$PM_{2.5}$ Kananaskis [a]	Smoke	13.11	1,112	**< 0.0005**
$R^2 = 0.189$	Year[Smoke]	3.16	4,112	**< 0.02**
	Month	1.08	1,112	> 0.3

K^+ [a]	Smoke	18.90	1,112	**< 0.0001**
$R^2 = 0.241$	Year[Smoke]	3.93	4,112	**< 0.005**
	Month	1.30	1,112	> 0.2
c) Rain chemistry				
K^+ mg/L [a]	Smoke	5.59	1,93	**0.0201**
$R^2 = 0.420$	Year[Smoke]	2.24	16,93	**< 0.009**
	Sample volume	18.80	1,93	**< 0.0001**
	Month	0.21	1,93	> 0.6
Ca^{2+} mg/L [a]	Smoke	9.15	1,93	**0.0005**
$R^2 = 0.547$	Year[Smoke]	3.86	16,93	**< 0.0001**
	Sample volume	33.20	1,93	**< 0.0001**
	Month	0.00	1,93	> 0.9
K^+/Ca^{2+} [a]	Smoke	0.02	1,94	>0.8
$R^2 = 0.305$	Year[Smoke]	2.55	16,94	**< 0.003**
	Sample volume	0.00	1,94	> 0.9
	Month	0.02	1,93	> 0.8
d) River chemistry				
K^+ mg/L	Smoke	24.51	1,130	**< 0.0001**
$R^2 = 0.818$	Year[Smoke]	37.52	15,130	**< 0.0001**
	Site	0.02	1,130	> 0.9
Ca^{2+} mg/L	Smoke	87.05	1,133	**< 0.0001**
$R^2 = 0.828$	Year[Smoke]	32.77	16,130	**< 0.0001**
	Site	36.25	1,130	**< 0.0001**
K^+/Ca^{2+}	Smoke	2.60	1,130	0.109
$R^2 = 0.798$	Year[Smoke]	33.92	15,130	**< 0.0001**
	Site	6.93	1,130	**< 0.01**
K^+/Ca^{2+} [b]	Smoke	17.15	1,128	**< 0.0001**
$R^2 = 0.882$	Year[Smoke]	62.75	15,128	**< 0.0001**
	Site	4.48	1,128	**< 0.05**

[a] ln-transformed, [b] excluding 2 outliers

3.2. Atmospheric particulate matter and chemistry

We considered $PM_{2.5}$ in Calgary (most years) and Kananaskis (six years) as our metrics of smoke in our study region. If smoke aerosols from long-range transport were present, we expected that PM2.5 in Calgary and Kananaskis would show similar patterns. In Calgary, $PM_{2.5}$ concentrations in July and August were approximately twice as high in smoke years than in no-smoke years (Figure 2b); there were no additional differences among years (Table 1b). August $PM_{2.5}$ values were higher than July $PM_{2.5}$ values in 16/18 years (Table 1b). Calgary $PM_{2.5}$ values for July and August across years were strongly predicted by the corresponding summed FRP values (Figure 3a; $R^2 = 0.805$, $F_{1,15} = 62.03$, $P < 0.0001$) demonstrating that regional wildfire is a major contributor to air quality in our study area. Air quality measured at the IMPROVE monitoring station in Kananaskis (2011-2016) was highly correlated with that in Calgary ($PM_{2.5}$: $r = 0.94$, $P < 0.0001$, $n = 275$ days). As observed for Calgary $PM_{2.5}$, Kananaskis $PM_{2.5}$ concentrations in July and August were higher in the smoke years (2014, 2015) than in the other years, consistent with long-range transport, with some variation among years within the smoke category but not between July and August (Table 1b).

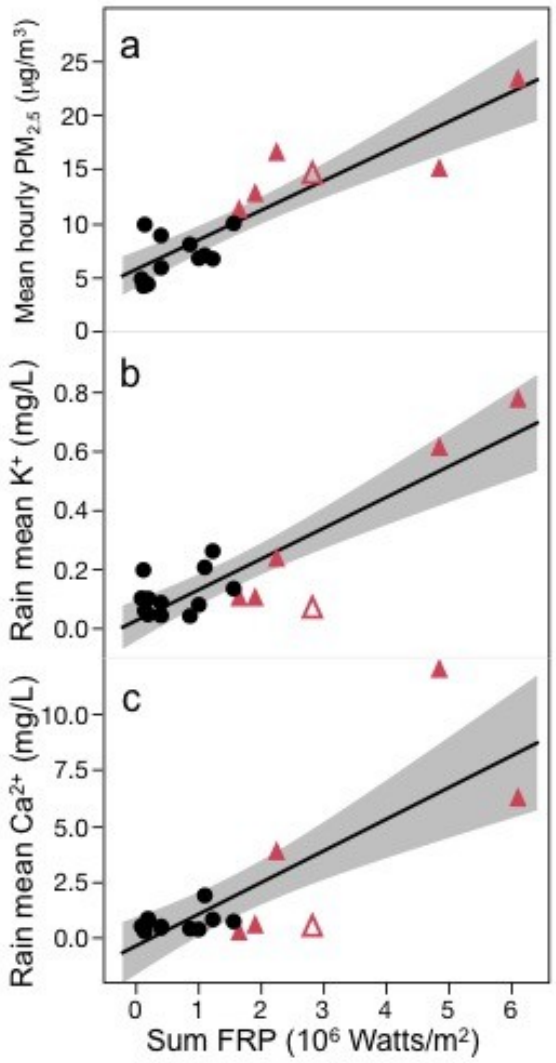

Figure 3. Mean values for July and August (combined) of (a) hourly Calgary $PM_{2.5}$ concentrations, (b) rain potassium, K^+, concentrations, (c) rain calcium, Ca^{2+}, concentrations in relation to fire activity in July and August (summed Fire Radiative Power values). Points are years from 2002-2019, red indicates smoke years with 2015 indicated by the open triangle.

Aerosol K^+ in $PM_{2.5}$, our primary marker of biomass combustion, was higher in smoke years than in no-smoke years (Figure 4a, Table 1b). Potassium increased strongly and exponentially with the quantity of Kananaskis $PM_{2.5}$ in absolute mass (Figure 5a, $\ln(K^+)$ vs. $PM_{2.5}$: $r = 0.96$, $n = 276$, $P < 0.0001$) and as a proportion of the measured constituents in aerosols (Figure 5b; polynomial: proportion $K^+ = 0.011+0.0048*\ln PM_{2.5} + 0.0078*(\ln PM_{2.5})^2$; all coefficients $P < 0.0001$, $R^2 =$

271 0.502, n = 276). Other constituents (n=10) reported in the IMPROVE data did not vary strongly
272 with $PM_{2.5}$ quantity (all $r < 0.44$), confirming that K^+ was the characteristic marker of biomass
273 combustion in air monitoring.

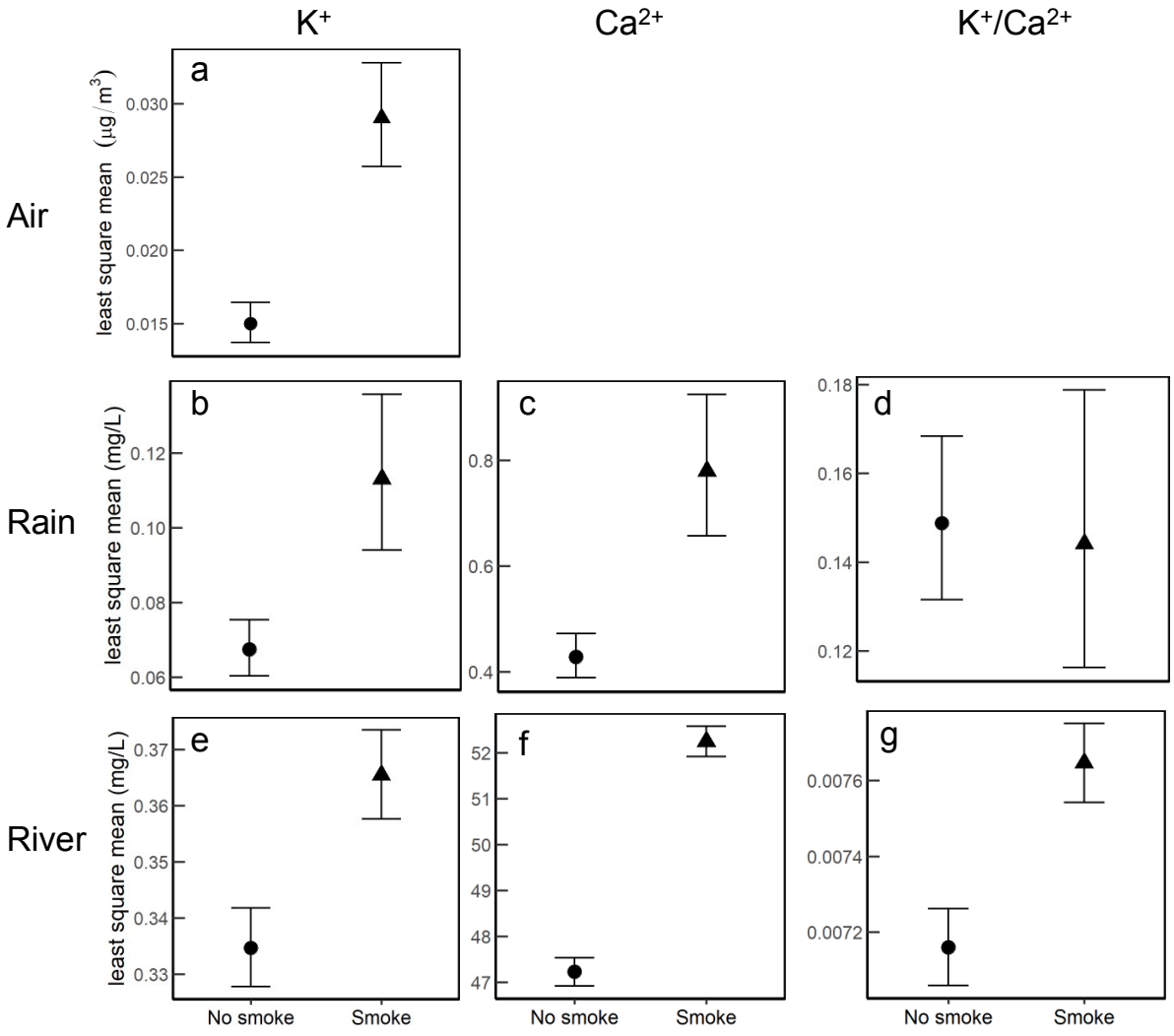

274

275 **Figure 4**. Least square means for no-smoke and smoke years from models in Table 1 for
276 potassium (K^+), calcium, (Ca^{2+}) and their ratio (unitless) in air, rain, and river water in the
277 Kananaskis watershed. Ca^{2+} was not available for air. Points are means ± SE, back-transformed
278 as appropriate.

279

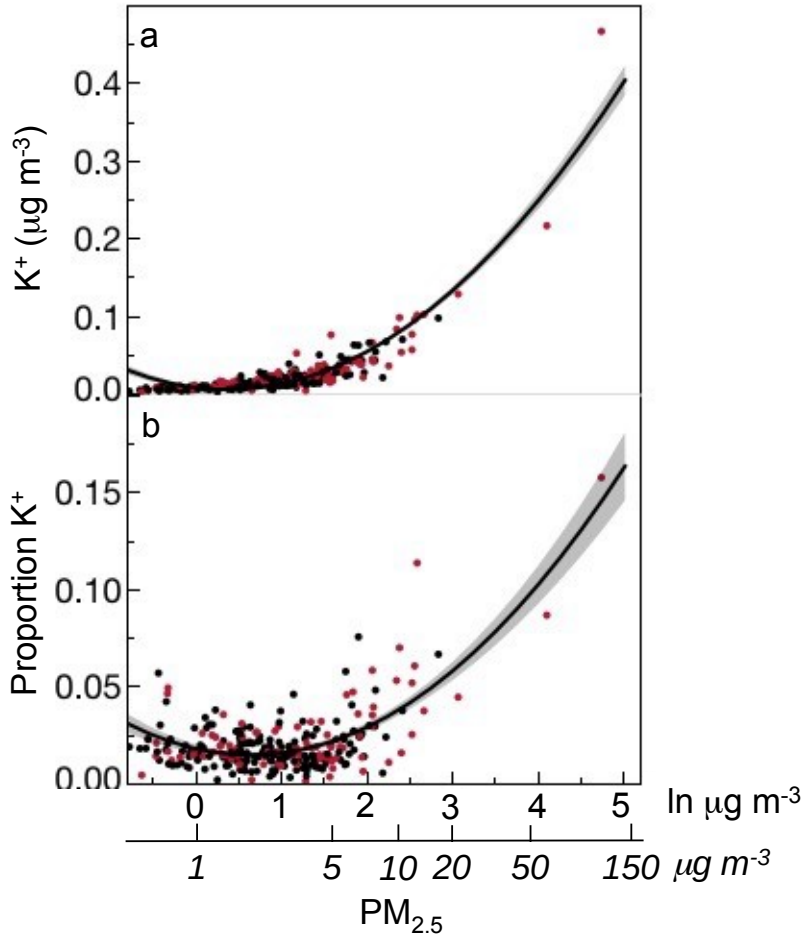

Figure 5. Absolute (a) and proportional (b) amount of potassium (K^+) in $PM_{2.5}$ as a function of $PM_{2.5}$ concentrations from the IMPROVE air sampling at Kananaskis. Red points indicate observations in smoky years. Fitted lines are shown with shaded 95% CI.

3.3 Rainfall quantity and chemistry

As would be expected, smoke years were drier than no-smoke years. In July and August, smoke years had fewer days with rain (mean 19.7 ± 2.9 days, n= 6; no-smoke years: 25.5 ± 1.4 days, n = 12; $F_{1,16} = 4.59$, $P < 0.05$) and less total rain (mean 87.1 ± 13.9 mm; no-smoke years: 138.1 ± 11.1 mm; $F_{1,16} = 7.51$, $P < 0.02$) than did no-smoke years. Years with fewer days of rain had less total rain ($r = 0.80$, n=18, $P < 0.0001$).

Rain in smoke years had higher concentrations of K^+ and Ca^{2+} than was seen in no-smoke years (Figure 4b,c, Table 1c). These conclusions account for the effect of sample volume (Table 1c), as rain solute concentrations typically decrease as rain volume increases. The ratio of K^+ to Ca^{2+} remained constant in smoke and no-smoke years (Figure 4d, Table 1c). The concentrations of both K^+ and Ca^{2+} in rain correlated directly with the amount of wildfire (summed FRP) in July and August (Figure 3b,c), indicating that smoke entered the ecosystem through wet deposition. One apparent exception was in 2015 (Figure 3, open triangle) where rain concentrations of K^+ and Ca^{2+} (Figure 3b,c) were much lower than expected based on FRP and PM2.5 values (Figure 3a) that we attribute to relatively heavy rain that year (see Discussion).

3.4 River discharge and chemistry

Water discharge at Opal was lower in smoke years (2.10 ± 0.30 m^3/s, $n = 6$) than in other years (2.98 ± 0.26 m^3/s, $n = 8$; $F_{1,12} = 4.96$, $P < 0.05$) and was positively correlated with total rainfall in July and August of the current year ($r = 0.58$, $n = 14$, $P < 0.03$). Lower discharge in smoke years was primarily due to lower water velocity (0.417 m/s vs. 0.502 m/s in no-smoke years, $F_{1,13} = 4.99$, $P < 0.05$) as river width and mean depth varied little between smoke and no-smoke years ($P > 0.4$ and >0.7, respectively). There was no detectable relationship between discharge and K^+ concentration (Figure 6a; $F_{1,12} = 0.10$, $P > 0.7$), including when the anomalously low 2015 K^+ values were excluded ($F_{1,11} = 3.76$, $P > 0.07$). Concentrations of Ca^{2+} were exceptionally low in two years (2002, 2004) with relatively high discharge (Figure 6b) resulting in a negative relationship between concentration and discharge when all years were included ($F_{1,13} = 9.58$, $P < 0.01$) but not when 2002 and 2004 were excluded ($F_{1,11} = 0.040$, $P > 0.8$). The ratio of K^+ to Ca^{2+} did not vary with discharge (Figure 6c; $F_{1,12} = 0.13$, $P > 0.7$, including if 2015 was excluded, $P > 0.5$).

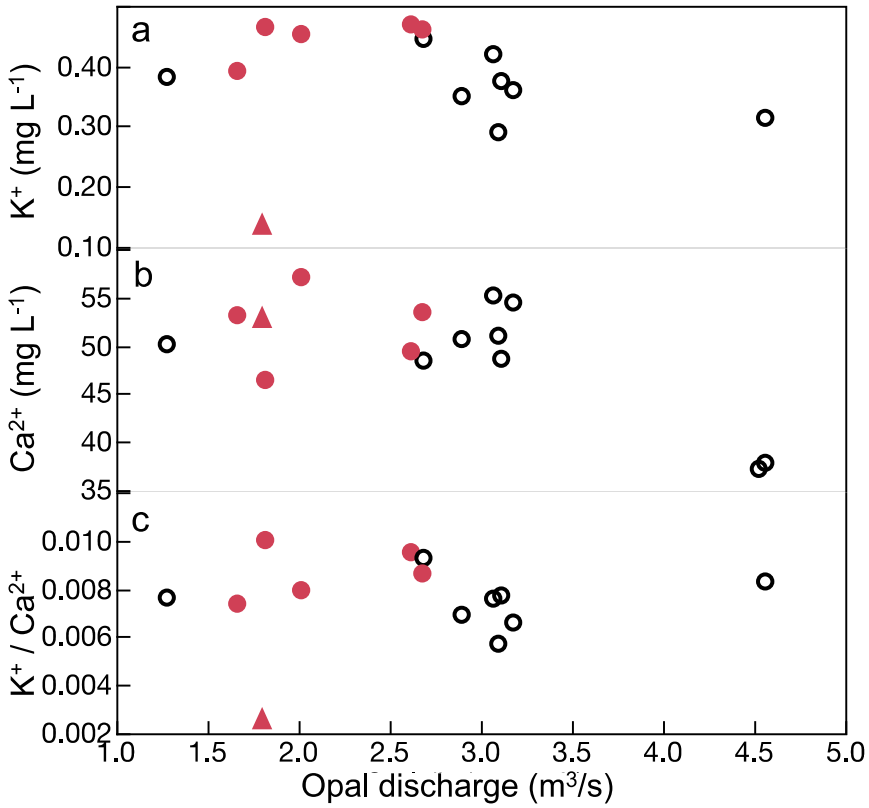

316

317 **Figure 6.** Kananaskis River mean concentrations of (a) potassium, K^+, (b) calcium, Ca^{2+}, and
318 (c) their ratio as a function of river discharge at the Opal site. Open black circles are no-smoke
319 years, red points are smoke years with 2015 indicated by the triangle.

320

321 In the Kananaskis River, smoke years had higher K^+ concentrations than in no-smoke years
322 (Table 1d), by an average of 0.031 mg/L or 9.2% of no-smoke years (Figure 4e, Table 2). There
323 was additional variation among years. Notably, 2015 had the lowest K^+ concentrations (simple
324 mean 0.136 $\pm$ 0.004 mg/L) of all the years in the study despite being a smoke year (Figure 3b).
325 Excluding 2015, river K^+ concentration in smoke years averaged 0.448 $\pm$ 0.008 mg/L (n = 57),
326 which was 28 % higher than in no-smoke years (0.335 $\pm$ 0.007 mg/L; n = 131).

327

328 Calcium concentrations in the river were also elevated in smoke years relative to other years
329 (Figure 4f, Table 1d), by 5.02 mg/L or 10.6% of no-smoke years. Unlike K^+, there were also

differences between sites, with Opal having more Ca^{2+} (LSM 51.0 $\pm$ 0.3 mg/L) than did KVB (48.5 $\pm$ 0.3 mg/L). In 2015, Ca^{2+} was not unusual (52.78 $\pm$ 0.45 mg/L, n = 12) compared to other smoke years (51.78 $\pm$ 0.55 mg/L, n = 57). Standardizing K^+ values relative to Ca^{2+} values (K^+/Ca^{2+}) revealed that K^+ increased more than Ca^{2+} in smoke years compared to other years (Figure 4g, Table 1d). This conclusion was sensitive to two observations in 2008 (a no-smoke year) at the KVB site that were highly influential (studentized residuals > 5). These had the highest K^+ values (0.59, 0.61 mg/L) that we observed in all years, and that were twice as high as the two other K^+ values from the same site and year. We have no explanation for these two extreme values and when they were omitted, there was a highly significant effect of smoke (Table 1d) with most smoke years having elevated K^+/Ca^{2+} values.

3.5 Atmospheric deposition model

Predicted concentrations of river K^+ in smoke and no-smoke years, and their difference, from our base model of deposition were very close to our observed values (Table 2). Predicted values were slightly lower than observed values, and our sensitivity analyses indicated that small (< 10%) increase in watershed area or decrease in river volume relative to our base values generated predicted values that gave the best match to observed values (Table S1). For deposition velocity, greater proportional changes resulted in smaller changes in predicted values than for watershed area and river volume because dry deposition contributed little relative to total deposition (Table S1). In our base model, wet deposition accounted for 93% and 96% of deposition in smoke and no-smoke years, respectively. Increasing $PM_{2.5}$ (dry) deposition velocity by four times (from 0.5 to 2 cm/s) resulted in wet deposition still accounting for the bulk of deposition (76% and 85% for smoke and no-smoke years, Table S1). Overall, the amount of

atmospheric deposition of K^+ appears sufficient to explain absolute concentrations of river K^+ as well as the difference between smoke and no-smoke years.

Table 2. Estimated contribution of atmospheric K^+ deposition (dry and wet) into the Kananaskis River watershed for the portion of the watershed between Lower Kananaskis Lake and the Opal sampling site for July and August in smoke and no-smoke years.

Variable	Smoke	No-smoke	Difference [a]
Dry deposition			
K^+ in air (ug/m3) [b]	0.029	0.015	0.014
K^+ deposition (kg) [c]	132.2	68.3	63.8
Wet deposition			
K^+ in rain (mg/L) [b]	0.113	0.067	0.046
Rain (L/m^2)	87.1	138.1	-51
K^+ deposition (kg) [c]	1673.2	1583.0	90.2
% wet deposition	92.7	95.9	-3.2
Total K^+ deposition (kg) [c]	1805.4	1651.4	154.0
K^+ in river (mg/L)			
Observed [b]	0.366 ± 0.008	0.335 ± 0.007	**0.031**
Predicted [d]	0.340	0.311	**0.029**

[a] Smoke years minus no-smoke years
[b] LSMs from Table 1, back-transformed (see Figure 1)
[c] for July and August in 170 km^2 watershed with deposition velocity of 0.5 cm/s
[d] for daily total K^+ deposition in $85.55*10^6$ L river water between Lower Kananaskis Lake and Opal.

4. Discussion

Distant fires affected the air quality in the Kananaskis Valley, southwest Alberta, in our study of six smoke years and 12 no-smoke years. We found that summer wildfire activity (FRP) across northwestern North America, but absent in southwest Alberta, strongly predicted concentrations of local $PM_{2.5}$ that also had elevated concentrations of K^+, a marker of biomass combustion. Rainwater had higher K^+ concentrations in smoke years than no-smoke years, and these concentrations were directly correlated with wildfire activity. The increased input of K^+ to the watershed by both dry ($PM_{2.5}$) and wet (precipitation) deposition was reflected in increased K^+ in the Kananaskis River in smoke years that closely matched the predicted concentrations from a simple model. Calcium, Ca^{2+}, also associated with biomass smoke but to a lesser extent than K^+ due to high inputs from mineral weathering (Sillanpää *et al*., 2005), was elevated in rainwater and river water in smoke years, but the ratio of K^+ to Ca^{2+} in river water was greater in smoke years. River discharge did not explain the differences between smoke and no-smoke years. Collectively, our study provides novel insights by demonstrating in a natural system that airborne pollutants can rapidly enter aquatic systems and that wildfires affect water quality even in unburned watersheds far from fires.

4.1 Time scale of river inputs

We found that the processes linking fire activity to river water quality were observable at an annual time scale, which is notable. Globally, approximately one third of river discharge consists of young water less than three months old (Jasechko *et al*., 2016). In steeper watersheds, such as the Kananaskis Valley, young water is predicted to be a smaller proportion (e.g. 20%) of discharge but generalities are constrained by limited data in mountainous terrain with winter snowpack (Campbell *et al*., 2020; Carroll *et al*., 2020; Jasechko *et al*., 2016). In our study, substantial contribution of young water to the river was evident in the positive correlation between river discharge at the Opal site in early September and the amount of rainfall in July and

August of the same year. Conversely, the contribution of Lower Kananaskis Lake to the river at Opal was difficult to discern. Discharge from the lake was either < 1 m^3/s or 24 m^3/s (power plant either off or on) while Opal discharge was much smaller and less variable, ranging 1.3 - 4.5 m^3/s. Among years, similar Opal discharges of approximately 3 m^3/s were observed whether there was either low or high discharge from the lake in the hours preceding stream gauging at Opal (data not shown). Further, concentrations of K^+ and Ca^{2+} in Lower Kananaskis Lake were much lower (< 3 mg/L and < 38 mg/L, respectively; Alberta Environment and Parks (2021)) than we observed in the river, likely reflecting the dominant contribution of snowmelt to the lake relative to summer rain; rain in the Kananaskis headwaters has higher concentrations of K^+ (3.2x) and Ca^{2+} (1.3x) than does snow (Lafrenière and Sinclair, 2011). Further work on the age of water in the Kananaskis River in late summer would be informative to understand the magnitude of rainwater inputs into river discharge.

Our results from 2015 provide some insight into the dynamics of K^+ in particular. This year was a smoke year as evident by fire activity and $PM_{2.5}$ concentrations in our study and elsewhere (Mirzaei *et al.*, 2018). However, rainfall concentrations of K^+ and Ca^{2+} were lower than expected (Figure 4b,c), and river concentrations of K^+, but not Ca^{2+}, were exceptionally low in 2015. We have no reason to doubt the validity of our measurements. The likely explanation is that 2015 had the highest rainfall (119 mm) in July and August of all the smoke years, including a single-day rainfall of 20 mm on 21 August that was in the top 1.5% of all daily rainfalls in our study period. There was no further rain before we sampled the river. We suggest that surface deposition and rainfall K^+ had been largely flushed from the watershed resulting in low river concentrations at the time of sampling. That Ca^{2+} did not show a similarly low concentration in 2015 is consistent with the greater contribution of rock weathering for Ca^{2+} compared to K^+.

4.2 Source of K^+ and Ca^{2+}

We focused on K^+ and Ca^{2+} as commonly sampled ions in water that are also associated with smoke from biomass combustion such as wildfires. Both ions can also derive from weathering of rock. The geology of the Kananaskis watershed is dominated by calcium carbonates (McMechan, 1995), with some potassium feldspar (Sharp *et al.*, 2002) of unknown abundance and distribution within the watershed. Water at our two sites differed in Ca^{2+} concentrations but not in K^+ concentrations, suggesting a larger weathering source for Ca^{2+} than for K^+. In rainwater, both K^+ and Ca^{2+} were elevated in smoke years compared to no-smoke years in equal proportions such their ratio did not differ between smoke and no-smoke years. Both ions were also elevated in river water in smoke years, but more so for K^+ than resulting in higher K^+/Ca^{2+} in smoke years than in no-smoke years. Atmospheric sources of Ca^{2+} contributing to river water Ca^{2+} would be minor relative to inputs from weathering, while for K^+, atmospheric deposition may be a dominant source (Lafrenière and Sinclair, 2011).

Variation in solute concentrations may also be affected by discharge, with the common expectation that increased discharge will be associated with reduced solute concentrations due to dilution. Many empirical studies have found no relationship between discharge and solute concentrations (chemostasis), while a global survey found support for a dilution effect for K^+ and Ca^{2+} (Botter *et al.*, 2020). We observed that smoke years had lower rainfall and river discharge than no-smoke years, but that concentrations of K^+ and Ca^{2+} and their ratio did not vary with discharge at the Opal site, i.e. it was chemostatic, as previously observed for K^+ but not for Ca^{2+} (Tripler *et al.*, 2006). Chemostatic behavior can occur when solutes are deposited on the surface rather than generated sub-surface (Botter *et al.*, 2020), supporting an atmospheric source for K^+

438 in our study. In the case of Ca^{2+}, weathering is dominant source in Kananaskis but variation in
439 its concentration appears largely buffered by ion exchange reactions occurring in the
440 groundwater zone as proposed for the adjacent Bow River (Grasby *et al.*, 1999). While the
441 many processes by which discharge affects solute concentrations in the Kananaskis River are
442 unquantified, our finding of higher K^+ and K^+ / Ca^{2+} in smoke years is more consistent with
443 atmospheric deposition rather than with dilution.
444
445 **4.3 Magnitude of smoke inputs**
446 We constructed a very simple model to relate atmospheric deposition to observed river
447 concentrations for K^+ using observed air and rain concentrations. Our predicted values matched
448 the observed values remarkably closely (Table 2) although many processes connecting the
449 atmosphere to the river were not considered. For example, dry deposition velocity of $PM_{2.5}$
450 varies widely with plant surface complexity and wind, as do retention and wash-off (Giardina
451 and Buffa, 2018; Schaubroeck *et al.*, 2014). However, dry deposition was a minor contribution
452 to total deposition in our model so its dynamics are not critical. Greater uncertainty applies to
453 the routes by which rain transports K^+ from the watershed to the river because losses may be
454 expected to groundwater and to uptake by plants while our model assumed all deposited K^+ in
455 July and August entered the river in the current year. It is likely that plant uptake of K^+ had
456 largely ceased by mid-July (Reid and Watson, 1966; Tripler *et al.*, 2006) such that deposited K^+
457 from wildfire would be available to reach the river. We conclude that K^+ in our system is
458 primarily from the atmosphere and that smoke explains the increased K^+ in the river in wildfire
459 years.
460

5. Conclusions

While direct effects of wildfires on water quality within burned watersheds are commonly studied, few studies have attempted to distinguish inputs from smoke that redistribute biomass constituents across a much wider geographic region than run-off from burned terrain. In our study of a wilderness river in an unburned watershed, most wildfires were hundreds of kilometers away. Nevertheless, we were able to track evidence of smoke from production (wildfire activity) through local air and rainfall chemistry to changes in river chemistry in six smoke years compared to 12 years without smoke. We did this using common ions, K^+ and Ca^{2+}, that are routinely measured in air and water quality analyses. While other compounds are more specifically associated with biomass smoke, e.g. levoglucosan, their very specificity reduces that the frequency and geographic extent of their measurement (Sullivan *et al.*, 2008). Elevated K^+ in water is not itself expected to be a concern for drinking water or ecosystem processes. However, K^+, which is commonly measured in air and water monitoring programs, could be a sentinel ion for the suite of nutrients, toxins and microbes in wildfire smoke that may originate far from a focal water body. Given the increasing frequency and intensity of wildfires, the contribution of wildfire smoke to the biogeochemistry of ecosystems and drinking water sources requires widespread assessment beyond the watersheds where wildfires occur.

Acknowledgments

We are indebted to Environmental Science students and staff of the University of Calgary for their assistance with field sampling, and to Farzin Malekani and Dorrie Wiwcharuk for water chemistry analyses. The staff of University of Calgary Biogeoscience Institute's Barrier Lake Field Station, especially Judy Buchanan-Mappin and Adrienne Cunnings, greatly facilitated field logistics and access to data, and we also thank government agencies for help with their data. Brian Gaas, Dylan Cunningham and Malvina Chmielarski provided valuable comments at early stages of this study.

Data Availability Statement

Datasets for this research are available in these in-text data citation references: (NASA, 2020) for fire activity, (Open Calgary, 2021) for Calgary air quality, (IMPROVE, 2021) for Kananaskis air quality and (University of Calgary Environmental Science Program, 2020) for river chemistry. Kananaskis rain chemistry and hydrology are available at https://dataverse.scholarsportal.info/privateurl.xhtml?token=844fefbe-ac6e-4e37-800c-7a37301630e9.

References

Alberta Environment and Parks (2021). Lake Water Quality Data. Lower Kananaskis Lake. https://www.alberta.ca/surface-water-quality-data.aspx. Last accessed 22 March 2021.

Alberta Government (2021). Alberta River Basins, Lower Kananaskis Lake (058F009). https://rivers.alberta.ca/. Last accessed 22 March 2021

Berthiaume, A., E. Galarneau, and G. Marson (2020). Polycyclic aromatic compounds (PACs) in the Canadian environment: Sources and emissions. *Environmental Pollution*, 116008. https://doi.org/10.1016/j.envpol.2020.116008

Botter, M., L. Li, J. Hartmann, P. Burlando, and S. Fatichi (2020). Depth of solute generation is a dominant control on concentration-discharge relations. *Water Resources Research, 56*(8), e2019WR026695. https://doi.org/10.1029/2019WR026695

Calgary Herald (2015). A timeline of smoky skies over Calgary. *Calgary Herald, Alberta,*

Campbell, É. M. S., I. Pavlovskii, and M. C. Ryan (2020). Snowpack disrupts relationship between young water fraction and isotope amplitude ratio; approximately one fifth of mountain streamflow less than one year old. *Hydrological Processes, 34*(25), 4762-4775. https://doi.org/10.1002/hyp.13914

Carroll, R. W. H., A. H. Manning, R. Niswonger, D. Marchetti, and K. H. Williams (2020). Baseflow age distributions and depth of active groundwater flow in a snow-dominated mountain headwater basin. *Water Resources Research, 56*(12), e2020WR028161. https://doi.org/10.1029/2020WR028161

Crosby, J. M. (1990), Kananaskis Lakes: Upper and Lower, in *Atlas of Alberta Lakes*, edited by P. Mitchell and E. Prepas, pp. 570-577, The University of Alberta Press, Edmonton, Alberta.

Dokas, I., M. Statheropoulos, and S. Karma (2007). Integration of field chemical data in initial risk assessment of forest fire smoke. *Science of the Total Environment, 376*(1-3), 72-85. https://10.1016/j.scitotenv.2007.01.064

Duck, T. J., et al. (2007). Transport of forest fire emissions from Alaska and the Yukon Territory to Nova Scotia during summer 2004. *Journal of Geophysical Research: Atmospheres, 112*, D10S44. https://10.1029/2006jd007716

Dupuy, J.-L., H. Fargeon, N. Martin-StPaul, F. Pimont, J. Ruffault, M. Guijarro, C. Hernando, J. Madrigal, and P. Fernandes (2020). Climate change impact on future wildfire danger and activity in southern Europe: a review. *Annals of Forest Science, 77*(2), 35. https://10.1007/s13595-020-00933-5

Giardina, M., and P. Buffa (2018). A new approach for modeling dry deposition velocity of particles. *Atmospheric Environment, 180*, 11-22. https://doi.org/10.1016/j.atmosenv.2018.02.038

Gilman, J. B., B. M. Lerner, W. C. Kuster, P. D. Goldan, C. Warneke, P. R. Veres, J. M. Roberts, J. A. de Gouw, I. R. Burling, and R. J. Yokelson (2015). Biomass burning emissions and potential air quality impacts of volatile organic compounds and other trace gases from fuels common in the US. *Atmospheric Chemistry and Physics, 15*(24), 13915-13938. https://10.5194/acp-15-13915-2015

Government of Canada (2021). Historical climate data. https://climate.weather.gc.ca/historical_data/search_historic_data_e.html

538 Grasby, S. E., I. Hutcheon, and L. McFarland (1999). Surface-water–groundwater interaction
539 and the influence of ion exchange reactions on river chemistry. *Geology, 27*, 223-226.
540 https://doi.org/10.1130/0091-7613(1999)027%3C0223:SWGIAT%3E2.3.CO;2

541 Halofsky, J. E., D. L. Peterson, and B. J. Harvey (2020). Changing wildfire, changing forests: the
542 effects of climate change on fire regimes and vegetation in the Pacific Northwest, USA. *Fire*
543 *Ecology, 16*(1), 4. https://10.1186/s42408-019-0062-8

544 Hung, W.-T., C.-H. Lu, B. Shrestha, H.-C. Lin, C.-A. Lin, D. Grogan, J. Hong, R. Ahmadov, E.
545 James, and E. Joseph (2020). The impacts of transported wildfire smoke aerosols on surface
546 air quality in New York State: A case study in summer 2018. *Atmospheric Environment,*
547 *227*, 117415. https://doi.org/10.1016/j.atmosenv.2020.117415

548 IMPROVE (2021). Interagency Monitoring of Protected Visual Environments.
549 https://vista.cira.colostate.edu/Improve

550 Jasechko, S., J. W. Kirchner, J. M. Welker, and J. J. McDonnell (2016). Substantial proportion
551 of global streamflow less than three months old. *Nature Geoscience, 9*(2), 126-129.
552 https://doi:10.1038/NGEO2636

553 Lafrenière, M. J., and K. E. Sinclair (2011). Snowpack and precipitation chemistry at a high
554 altitude site in the Canadian Rocky Mountains. *Journal of Hydrology, 409*(3), 737-748.
555 https://doi.org/10.1016/j.jhydrol.2011.09.007

556 Liu, J. C., L. J. Mickley, M. P. Sulprizio, F. Dominici, X. Yue, K. Ebisu, G. B. Anderson, R. F.
557 A. Khan, M. A. Bravo, and M. L. Bell (2016). Particulate air pollution from wildfires in the
558 Western US under climate change. *Climatic Change, 138*(3-4), 655-666.
559 https://10.1007/s10584-016-1762-6

560 McMechan, M. E. (1995), Geology of the Rocky Mountain Foothills and Front Ranges in
561 Kananaskis Country, Alberta. Map 1865A, Geological Survey of Canada,.

562 Mirzaei, M., S. Bertazzon, and I. Couliogner (2018). Modeling wildfire smoke pollution by
563 integrating land use regression and remote sensing data: Regional multi-temporal estimates
564 for public health and exposure models. *Atmosphere, 9*, 1-18.
565 https://doi.org/10.3390/atmos9090335

566 Moore, R. A., C. Bomar, L. N. Kobziar, and B. C. Christner (2021). Wildland fire as an
567 atmospheric source of viable microbial aerosols and biological ice nucleating particles. *The*
568 *ISME Journal, 15*(2), 461-472. https://10.1038/s41396-020-00788-8

569 Munchak, L. A., B. A. Schichtel, A. P. Sullivan, A. S. Holden, S. M. Kreidenweis, W. C. Malm,
570 and J. L. Collett (2011). Development of wildland fire particulate smoke marker to organic

carbon emission ratios for the conterminous United States. *Atmospheric Environment, 45*(2), 395-403. https://10.1016/j.atmosenv.2010.10.006

NASA (2020). Fire Information For Resource Management System (FIRMS). https://firms.modaps.eosdis.nasa.gov/.

Nunes, B., V. Silva, I. Campos, J. L. Pereira, P. Pereira, J. J. Keizer, F. Goncalves, and N. Abrantes (2017). Off-site impacts of wildfires on aquatic systems - Biomarker responses of the mosquitofish *Gambusia holbrooki*. *Science of the Total Environment, 581-582*, 305-313. https://10.1016/j.scitotenv.2016.12.129

Open Calgary (2021). Historical air quality by parameter. https://data.calgary.ca/Environment/Historical-air-quality-by-parameter/7g8h-ukcq

R Core Team (2018). R: A language and environment for statistical computing. *R Foundation for Statistical Computing,*

Raison, R. J., P. K. Khanna, and P. V. Woods (1985). Mechanisms of element transfer to the atmosphere during vegetation fires. *Canadian Journal of Forest Research, 15*, 132-140. https://doi.org/10.1139/x85-022

Reid, R. W., and J. A. Watson (1966). Sizes, distributions, and numbers of vertical resin ducts in lodgepole pine. Periodical Sizes, distributions, and numbers of vertical resin ducts in lodgepole pine, 44, 519-525, doi: DOI.

Robinne, F.-N., K. D. Bladon, U. Silins, M. B. Emelko, M. D. Flannigan, M.-A. Parisien, X. Wang, S. W. Kienzle, and D. P. Dupont (2019). A regional-scale index for assessing the exposure of drinking-water sources to wildfires. *Forests, 10*(5), 384. https://10.3390/f10050384

Santín, C., S. H. Doerr, X. L. Otero, and C. J. Chafer (2015). Quantity, composition and water contamination potential of ash produced under different wildfire severities. *Environmenatal Research, 142*, 297-308. http://10.1016/j.envres.2015.06.041

SAS (2015), JMP 12.0.1., edited, SAS Institute Inc., Cary, NC, USA.

Schaubroeck, T., G. Deckmyn, J. Neirynck, J. Staelens, S. Adriaenssens, J. Dewulf, B. Muys, and K. Verheyen (2014). Multilayered modeling of particulate matter removal by a growing forest over time, from plant surface deposition to washoff via rainfall. *Environmental Science & Technology, 48*(18), 10785-10794. https://10.1021/es5019724

Schweizer, D., R. Cisneros, and M. Buhler (2019). Coarse and fine particulate matter components of wildland fire smoke at Devils Postpile National Monument, California, USA. *Aerosol and Air Quality Research, 19*(7), 1463-1470. https://doi: 10.4209/aaqr.2019.04.0219

Sharp, M., R. A. Creaser, and M. Skidmore (2002). Strontium isotope composition of runoff from a glaciated carbonate terrain. *Geochimica et Cosmochimica Acta, 66*, 595-614. https://doi.org/10.1016/S0016-7037(01)00798-0

Sillanpää, M., S. Saarikoski, R. Hillamo, A. Pennanen, U. Makkonen, Z. Spolnik, R. Van Grieken, T. Koskentalo, and R. O. Salonen (2005). Chemical composition, mass size distribution and source analysis of long-range transported wildfire smokes in Helsinki. *Science of the Total Environment, 350*(1-3), 119-135. https://10.1016/j.scitotenv.2005.01.024

Smith, A. J. P., M. W. Jones, J. T. Abatzoglou, J. G. Canadell, and R. A. Betts (2020). Climate change increases the risk of wildfires: September 2020. *ScienceBrief Review*. https://doi.org/10.5281/zenodo.4570195

Spencer, C. N., and F. R. Hauer (1991). Phosphorus and nitrogen dynamics in streams during a wildfire. *Journal of the North American Benthological Society, 10*, 24-30

Sullivan, A. P., A. S. Holden, L. A. Patterson, G. R. McMeeking, S. M. Kreidenweis, W. C. Malm, W. M. Hao, C. E. Wold, and J. L. Collett (2008). A method for smoke marker measurements and its potential application for determining the contribution of biomass burning from wildfires and prescribed fires to ambient $PM_{2.5}$ organic carbon. *Journal of Geophysical Research, 113*(D22). http://10.1029/2008jd010216

Tripler, C. E., S. S. Kaushal, G. E. Likens, and W. M. Todd (2006). Patterns in potassium dynamics in forest ecosystems. *Ecology Letters, 9*(4), 451-466. https://10.1111/j.1461-0248.2006.00891.x

University of Calgary Environmental Science Program (2020). Lower Kananaskis River (Alberta) water monitoring (dataset). Accessed from DataStream. https://doi.org/10.25976/b9zx-bd54

Valerino, M. J., J. J. Johnson, J. Izumi, D. Orozco, R. M. Hoff, R. Delgado, and C. J. Hennigan (2017). Sources and composition of PM2.5 in the Colorado Front Range during the DISCOVER-AQ study. *Journal of Geophysical Research: Atmospheres, 122*(1), 566-582. https://10.1002/2016jd025830

Verma, V., A. Polidori, J. J. Schauer, M. M. Shafer, F. R. Cassee, and C. Sioutas (2009). Physicochemical and toxicological profiles of particulate matter in Los Angeles during the October 2007 southern California wildfires. *Environmental Science & Technology, 43*, 954-960. https://doi.org/10.1021/es8021667

Whitfield, P. H. (2014). Climate station analysis and fitness for purpose assessment of 3053600 Kananaskis, Alberta. *Atmosphere-Ocean, 52*(5), 363-383. https://10.1080/07055900.2014.946388

Yu, P., et al. (2019). Black carbon lofts wildfire smoke high into the stratosphere to form a persistent plume. *Science, 365*, 587-590. https://doi.org/10.1126/science.aax1748